ChemComm

Accepted Manuscript

This article can be cited before page numbers have been issued, to do this please use: X. Shen, B. Song, B. Fang, A. Jiang, S. Ji and Y. He, *Chem. Commun.*, 2018, DOI: 10.1039/C8CC00047F.

ROYAL SOCIETY OF CHEMISTRY

rsc.li/chemcomm

View Article Online
DOI: 10.1039/C8CC00047F

Journal Name

COMMUNICATION

Excitation-Wavelength-Dependent Photoluminescence of Silicon Nanoparticles Enabled by Adjustment of Surface Ligands

Received 00th January 20xx,
Accepted 00th January 20xx

DOI: 10.1039/x0xx00000x

www.rsc.org/

Xiao-Bin Shen,[¶,§] Bin Song,[‡,§] Bei Fang,[‡] Ai-Rui, Jiang,[‡] Shun-Jun Ji,*[,¶] and Yao He*[,‡]

We herein present pioneering studies to reveal that excitation-wavelength-dependent photoluminescence property of fluorescent silicon nanoparticles (SiNPs) can be realized by rationally designing surface ligand, i.e., several kinds of oxidized indole derivatives. The resultant ligands-decorated SiNPs exhibit strong fluorescence, with significant excitation-wavelength-dependent emissive shifting from ~420 nm to ~550 nm. Taking advantages of their unique optical merits, we further exploit the resultant ligands-decorated SiNPs as novel fluorescent labels for anti-counterfeiting and cell imaging.

As the most important zero-dimensional silicon nanomaterial, silicon nanoparticles (SiNPs) have received intensive attention and shown high promise for myriad optical applications due to their attractive optical properties and negligible toxicity.[1,2] Over the past two decades, extensive efforts have been made for synthesizing high-performance fluorescent SiNPs.[3] It is worthwhile to mention that, recent studies have revealed that surface ligands attached to SiNPs play significant roles in optical properties of SiNPs. In particular, the ligands containing nitrogen atoms (e.g., N-H group) have a large impact on the fluorescent properties of SiNPs.[4] To date, highly luminescent SiNPs have been successfully achieved through modifying surface of SiNPs with proper ligands (e.g., diphenylamine, carbazole, 1,2,3,4-tetrahydrocarbazol-4-one, and Cy dye series[4]). Despite above-mentioned tremendous achievement, there still exists challenge to rationally control emission spectra of SiNPs through the adjustment of their surface ligands.

Herein, we reveal that distinct excitation-wavelength-dependent photoluminescence (PL) of SiNPs could be readily realized via introducing new kinds of surface ligands, i.e., oxidized indole derivatives. Taken together with the measurement of photoluminescent energy and time-correlated single photon counting (TCSPC), we deduce that photoexcited charge transfer process in different gap states is responsible for the observed excitation-wavelength-dependent PL. Taking advantage of the unique optical features, we further employ the resultant SiNPs for anti-counterfeiting and cell imaging applications.

In our experiment, the design of the surface ligands is based on the following considerations. (1) The indole is the core structure in many optoelectronic molecules and natural products, which shows excellent photoelectric activity and favourable biocompability.[5] (2) The indole possesses a nitrogen-containing aromatic electron-rich molecular system, providing the feasibility for improving and modulating the PL properties of SiNPs.[4a] It is worth noting that surface modification with indole molecule produces little influence on the maximum emission wavelength of SiNPs (Fig. S1). The reason is that compared to N-H group, the C3 site possesses more reactive position of indole towards electrophilic substitution, thus hindering the introduction of nitrogen defect.[5a] Therefore, with an aim to efficiently introduce nitrogen defect, the indole molecule is passivated through the I_2/TBHP mediated oxidation reaction, producing four kinds of oxidized indole derivatives.[5b,c] These resultant oxidized indole molecules are then used for modifying the SiNPs surface.

The chemical structures of the as-synthesized oxidized indole molecules are listed in Scheme 1b, namely isatin, 4-methylisatin, (*E*)-*N*-(*p*-tolyl)-3-(*p*-tolylimino)-3*H*-indol-2-amine, and (*E*)-6-methyl-*N*-(*p*-tolyl)-3-(*p*-tolylimino)-3*H*-indol-2-amine, which are respectively shorted for IST, MIST, TTIA, and MTTIA, (see corresponding NMR characterizations in Fig. S2-S4). The ligand-decorated SiNPs are formed through a two-step process (Scheme 1a). Non-ligand decorated SiNPs (i.e., NH_2-SiNPs) are

[¶]*Key Laboratory of Organic Synthesis of Jiangsu Province, College of Chemistry, Chemical Engineering and Materials Science, Soochow University, Suzhou 215123, China*
[‡]*Jiangsu Key Laboratory for Carbon-Based Functional Materials and Devices, Institute of Functional Nano & Soft Materials (FUNSOM), and Collaborative Innovation Center of Suzhou Nano Science and Technology (NANO-CIC), Soochow University, Suzhou, Jiangsu 215123, China*
[§]*These authors contribute equally.*
E-mail: yaohe@suda.edu.cn; shunjun@suda.edu.cn
† Electronic Supplementary Information (ESI) available: Materials and devices, methods, additional data (Fig. S1-S15), and corresponding discussions. See DOI:10.1039/x0xx00000x

View Article Online
DOI: 10.1039/C8CC00047F

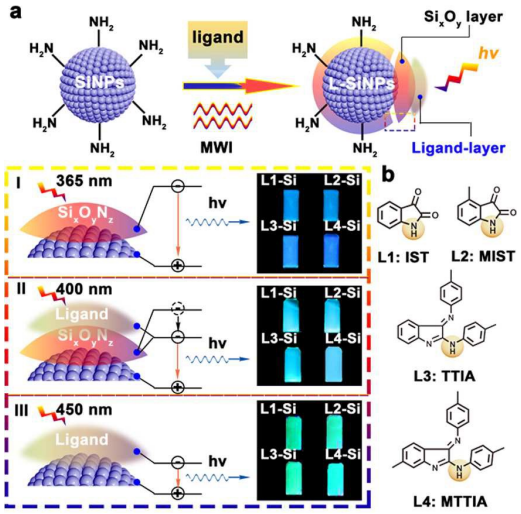

Scheme 1. (a) Schematic illustration of synthesis of ligand-decorated SiNPs. Dashed line frame presents a proposed mechanism for excitation-wavelength-dependent fluorescent property of the SiNPs: the photon production originates from exciton radiative recombination in different gap states under different excitation wavelengths, resulting in the excitation wavelength-dependent emission property of SiNPs. (b) Chemical structures of the as-synthesized oxidized indole molecules.

firstly formed under microwave irradiation via Ostwald ripeningprocess.[6] The resultant SiNPs are then modified by the above-mentioned ligands through self-assembly process.[4a,b,c] Meanwhile, the surface of SiNPs is prone to be partially oxidized to yield silica shell due to easy oxidization of silicon in the ambient environment. Of particular significance, the as-prepared SiNPs exhibit excitation-wavelength-dependent PL property, as shown in the frame in Scheme 1a. (I) When excited at 365 nm, the resultant SiNPs emit strong blue light. According to the energy gap law, the observed blue luminescence could be attributed to the radiative recombination of excitons in a charge transfer (CT) state at the Si/SiO_xN_y interface.[4b,e] (II) Cyan luminescence is observed under 400 nm excitation. The red-shift phenomenon of PL peak indicates the formation of a lower energy gap, which might be localized in the interface of SiO_xN_y/ligand. This result suggests the successful introduction of nitrogen defect. (III) Green luminescence is visible under the excitation wavelength of 450 nm. In this case, the blue PL is quenched due to the mismatch between the excitation and emission wavelength (excitation wavelength is larger than emission wavelength). As shown in Fig. S5, the free ligands show a maximum emission peak at ~530 nm through the microwave treatment; similarly, the ligand-decorated SiNPs exhibit a ~530 nm maximum emission peak when excited by ~450 nm. These results indicate that the green PL of SiNPs is attributed by ligand effect.

Transmission electron microscopy (TEM) image (Fig. 1a) shows that the as-prepared IST-SiNPs are well-monodispersed with a spherical structure and an average particle size of ~4.7 nm (Fig. 1a-insert). A high-resolution TEM image (HRTEM) (Fig. 1b) shows clear lattice spacing of ~0.31 nm for a single SiNP, corresponding to the (111) facet of Si.[4a,d] Moreover, as shown in the selected-area electron diffraction pattern (Fig. 1b-insert), the set of spots with a lattice spacing of ~0.31 nm are ascribed to the (111) reflection of silicon, demonstrating good crystallinity of the resultant SiNPs. The normalized UV-PL spectra (Fig. S6a) show a resolved absorption peak at ~310 nm and a PL peak at ~430 nm (excitation wavelength: 370 nm). From the UV-vis absorption spectral analysis (Fig. S6b), we deduce that the ~310 nm absorption in IST-SiNPs is produced by the ligand. This result suggests the successful introduction of ligand into SiNPs. Furthermore, the surface ligand of SiNPs is characterized by Fourier Transform Infrared (FT-IR) spectra (Fig. 1c), in which the characteristic stretching of the C=C bond (*ca.* ~1640 cm^{-1}) is observed for both the ligand and SiNPs. The strong and sharp absorbance peak at ~1030 cm^{-1}, which is attributed to Si-O-Si[4a-c], suggests the high oxidation state of SiNPs. The EDX data confirms the existence of Si in the SiNPs (Fig. S6c), and the oxidation state is further verified by X-ray photoemission spectroscopy (XPS). As shown in Fig. 1d, the emissions at 99.4, 100.4, 101.4, 102.4 and 103.4 eV are assigned to Si(0), Si(I), Si(II), Si(III) and Si(IV), respectively.[4a,b] The appearance of the Si(0) peak also confirms the existence of a silicon core. Taken together, these results suggest the SiNPs have a crystalline Si/SiO_xN_y core/shell structure, whose surface is covered by IST ligands. Significantly, the as-prepared SiNPs exhibit excitation-wavelength-dependent PL property (Fig. 1e). Typically, the emission peaks shift from ~415 to 550 nm with the increase of excitation wavelength from 350 to 520 nm, respectively. In the short excitation wavelength window (350-370nm), the emission intensity is enhanced with no obvious red-shift phenomenon, while gradually diminishes

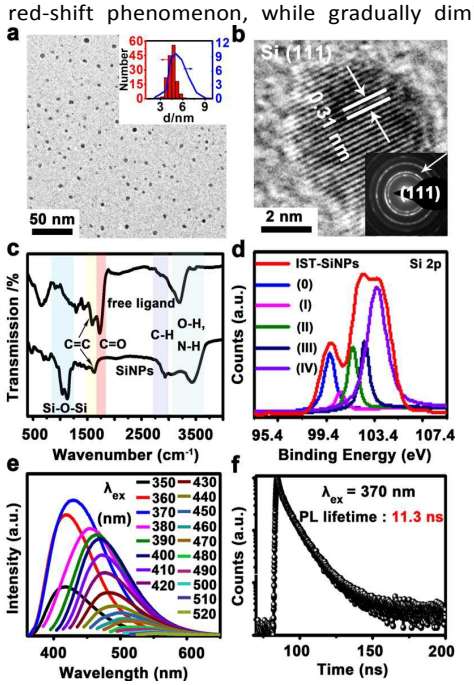

Fig. 1 (a) TEM image of the IST-SiNPs; the inset shows the TEM size deviation (4.7 ± 0.6 nm) and DLS diameter (~5.1 nm) of the

View Article Online
DOI: 10.1039/C8CC00047F

SiNPs. (b) HRTEM image of a single SiNP; the insert shows selected-area electron diffraction pattern. (c) FT-IR spectra of free ligand (IST) and resultant SiNPs; (d) X-ray photoemission spectra of Si 2p region; (e) Excitation-wavelength-dependent emission spectra of IST-SiNPs; (f) TCSPC spectrum of IST-SiNPs (λ_{ex} = 370 nm; λ_{em} = 430 nm, 25 °C).

in the long excitation wavelength window. Previous study reveals that in the short excitation window, the σ* → n transition produced by the surface functional groups (e.g., -OH/NH_2) leads to the strong blue emission of SiNPs. With the excitation wavelength increases, the π* → π transition contributed by the ligands is favored.[7] Therefore, the surface functional groups and ligands could act as the surface trap states, which contribute to the observed excitation-wavelength-dependent PL. The PL lifetime of the SiNPs is 11.3 ns at 370 nm excitation, which is measured by time-correlated single photon counting (TCSPC) technique (Fig. 1f). This nanosecond-scale emission further demonstrates that the PL is arisen from CT state,[4d,e] which allows fast radiative exciton recombination.

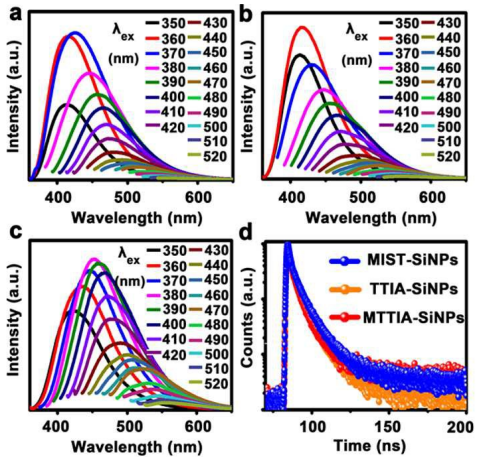

Fig. 2 Excitation-wavelength-dependent PL spectra of (a) MIST-SiNPs; (b) TTIA-SiNPs; (c) MTTIA-SiNPs. (d) TCSPC spectra of the resultant SiNPs (λ_{ex} = 370 nm; λ_{em} = emission maximum wavelength, 25 °C).

To test the generality of the ligand effect, other three kinds of ligands are also employed for modifying SiNPs. The characterization data for the resultant SiNPs are presented in Fig. S7-9. Notably, all of the resultant SiNPs exhibit similar excitation-wavelength-dependent PL property, as shown in Fig. 2a-c. The emission region ranges from ~420 nm to ~550 nm, and the normalized PL spectra are displayed in Fig. S10. Furthermore, the values of PL lifetimes are determined as 16.7, 8.7, and 14.6 ns under 370 nm excitation (Fig. 2d). The fluorescent quantum yields (QYs) are calculated as 12%, 20%, 8%, and 16% for IST-, MIST-, TTIA, and MTTIA-SiNPs, respectively (Fig. S11). Longer fluorescent lifetime is found to be related to higher QY in these SiNPs, which suggests the radiative recombination process can be promoted by the electron-richer ligands.[4a,8] To interrogate the mechanism of the observed excitation-wavelength-dependent PL property, a control experiment is performed, in which the silicon source (i.e., APTMS) is absence during the microwave irradiation reaction. The resultant materials exhibit the maximum emission peak at ~530 nm, while show excitation-wavelength-independent PL property (Fig. S5). Also, the products displays feeble fluorescence, whose intensity is much weaker than that of the ligand-decorated SiNPs. Besides, the excitation-wavelength-dependent PL property could not be observed in the absence of ligands (Fig. S12). Moreover, the PL lifetimes of the resultant SiNPs excited at 450 nm are slightly shorter than those excited at 370 nm (Fig. S13). This result is different from the excitation-wavelength-independent NH_2-SiNPs, whose PL lifetime dramatically decreases from 10.8 ns (370-nm excitation) to 1.9 ns (450-nm excitation) (Fig. S14), indicating that the resultant ligand-decorated SiNPs feature different pathways for the recombination of electrons and holes.[4a] Taken together, we deduce that the excitation-wavelength-dependent PL property is ascribed to the different CT states during ligand-actived process, thus producing the multiple energy levels in the band gap of SiNPs and generating excitation-wavelength-dependent emission property (Scheme 1).

Taking advantages of unique optical properties (e.g., excitation wavelength-dependent emission, as well as the superior photostability against long-term high-power UV irradiation (Fig. S15)), we further exploit the resultant SiNPs for anti-counterfeiting applications. Assisted by inkjet printing technique[9], silicon-based fluorescent ink is applied for pattern printing (please see the detailed preparation of the ink and instrument setup in ESI). Figure 3a displays the fluorescent images of the butterfly-patterned paper printed by IST-SiNPs. Blue, green, and yellow fluorescent images are observed, when excited at 360, 455, and 523 nm, respectively. Quick Response (QR) patterns (Fig. 3b (I)-(III)) are also readable under different excitation wavelength. Furthermore, the SiNP- and R6G-ink are simultaneously used to improve the anti-

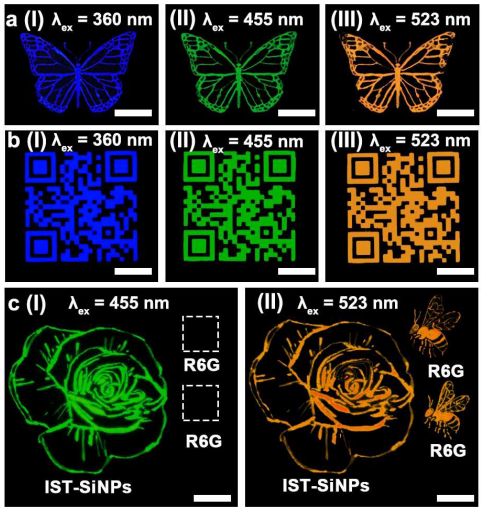

Fig. 3 Fluorescent images of patterned commercially available papers labeled with IST-SiNPs through inkjet printing. (a) Butterfly-patterned images captured with excitation at: (I) 360 nm, (II) 455 nm, and (III) 523 nm. (b) Quick Response (QR)-

View Article Online
DOI: 10.1039/C8CC00047F

patterned images captured with excitation at: (I) 360 nm, (II) 455 nm, and (III) 523 nm. (c) Rose- and bees-patterned images composed from SiNP- and Rhodamine 6G (R6G)-solution captured with excitation at: (I) 455 nm, (II) 523 nm. Blue emission window: 460-490 nm, exposure time: 800 ms; green emission window: 490-520 nm, exposure time: 2000 ms; yellow emission window: 540-590 nm, exposure time: 5000 ms. The thick white lines correspond to 1 cm.

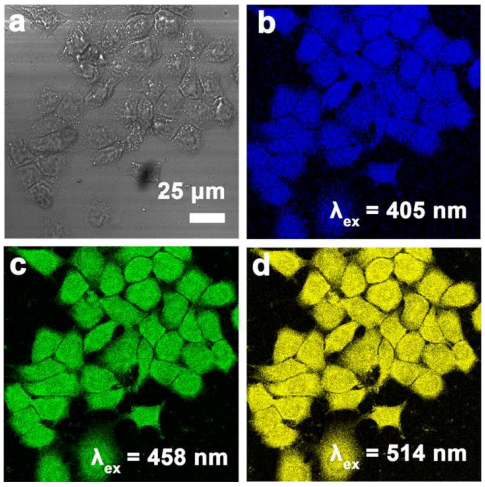

Fig. 4 Confocal images of HeLa cells distributed with the IST-SiNPs. (a) Bright-field image. Cell images under excitation at (b) 405 nm, emission band pass: 430-470 nm; (c) 458 nm, emission band pass: 470-510 nm; (d) 514 nm, emission band pass: 530-570 nm.

counterfeiting efficacy. In our case, rose and bees are coated with IST-SiNPs and R6G, respectively. As shown in Fig. 3c, upon excitation at 455 nm, only the rose printed by SiNP-ink appears in the pattern, while bees printed by R6G-ink are invisible (Fig. 3c (I)). When excited at 523 nm, yellow fluorescent signals from both SiNPs and R6G are readily observed in the whole pattern (Fig. 3c (II)). In addition to anti-counterfeiting applications, these ligand-modified fluorescent SiNPs also show potential feasibility for bioimaging applications. As proof-of-concept demonstration, the fixed Hela cells distributed with SiNPs exhibit strong and resolved fluorescent signals. As shown in Fig. 4, obvious blue, green, and yellow fluorescent images are observed upon excitation at 405, 458, and 514 nm, respectively.

Conclusions

In summary, we develop a kind of fluorescent SiNPs featuring excitation-wavelength-dependent PL property, based on introducing oxidized indole derivatives as surface ligands. Taken together with the PL energy and TCSPC results, we deduce the origin of the excitation-wavelength-dependent fluorescent property is mainly attributed to the formation of different CT states. We further exploit the resultant SiNPs as novel fluorescent labels for anti-counterfeiting and bioimaging applications. These results offer valuable information for rationally designing high-quality SiNPs with unique optical merits and understanding their luminescent mechanism, facilitating the promotion of SiNPs-based widespread applications (e.g., laser, catalysis, solar cells, sensing and bioimaging, etc.).

We express our thanks for the financial support provided by National Basic Research Program of China (973 Program 2013CB934400), the National Natural Science Foundation of China (21672157, 21542015, 21372174, 61361160412, 31400860, 21575096, and 21605109), the Ph.D. Programs Foundation of the Ministry of Education of China (2013201130004), the Priority Academic Program Development of Jiangsu Higher Education Institutions (PAPD), 111 Project, and the Collaborative Innovation Center of Suzhou Nano Science and Technology (NANO–CIC).

Notes and references

1 (a) J. H. Park, L. Gu, G. v. Maltzahn, E. Ruoslahti, S. N. Bhatia, M. J. Sailor, *Nature Mater.*, 2009, **8**, 331-336; (b) L. Gu, D. J. Hall, Z. T. Qin, E. Anglin, J. Joo, D. J. Mooney, S. B. Howell, M. J. Sailor, *Nature Commun.*, 2013, **4**, 2326; (c) J. W. Liu, F. Erogbogbo, K. T. Yong, L. Ye, J. Liu, R. Hu, H. Y. Chen, Y. Z. Hu, Y. Yang, J. H. Yang, I. Roy, N. A. Karker, M. T. Swihart, P. N. Prasad, *ACS Nano*, 2013, **7**, 7303-7310.

2 (a) F. Peng, Y. Y. Su, Y. L. Zhong, C. H. Fan, S. T. Lee, Y. He, *Acc. Chem. Res.*, 2014, **47**, 612-623; (b) Y. Y. Su, X. Y. Ji, Y. He, *Adv. Mater.*, 2016, **28**, 10567-10574.

3 (a) A. G. Cullis, L. T. Canham, *Nature*, 1991, **353**, 335-338; (b) B. F. P. McVey, R. D. Tilley, *Acc. Chem. Res.*, 2014, **47**, 3045-3051; (c) X. Y. Cheng, S. B. Lowe, P. J. Reece, J. J. Gooding, *Chem. Soc. Rev.*, 2014, **43**, 2680-2700; (d) M. Dasog, J. Kehrle, B. Rieger, J. G. C. Veinot, *Angew. Chem. Int. Ed.*, 2016, **55**, 2322-2339; (e) T. Yu, F. Wang, Y. Xu, L. L. Ma, X. D. Pi, D. R. Yang, *Adv. Mater.*, 2016, **28**, 4912-4919.

4 (a) Q. Li, Y. He, J. Chang, L. Wang, H. Z. Chen, Y. W. Tan, H. Y. Wang, Z. Z. Shao, *J. Am. Chem. Soc.*, 2013, **135**, 14924-14927; (b) Q. Li, T. Y. Luo, M. Zhou, H. Abroshan, J. C. Huang, H. J. Kim, N. L. Rosi, Z. Z. Shao, R. C. Jin, *ACS Nano*, 2016, **10**, 8385-8393; (c) Y. L. Zhong, B. Song, F. Peng, Y. Y. Wu, S. C. Wu, Y. Y. Su, Y. He, *Chem. Commun.*, 2016, **52**, 13444-13447; (d) M. Dasog, Z. Y. Yang, S. Regli, T. M. Atkins, A. Faramus, M. P. Singh, E. Muthuswamy, S. M. Kauzlarich, R. D. Tilley, J. G. C. Veinot, *ACS Nano*, 2013, **7**, 2676-2685; (e) G. De los Reyes, M. Dasog, M. Na, L. Titova, J. G. C. Veinot, F. A. Hegmann, *Phys. Chem. Chem. Phys.*, 2015, **17**, 30125-30133.

5 (a) M. Bandini, A. Eichholzer, *Angew. Chem. Int. Ed.*, 2009, **48**, 9608-9644; (b) Z. J. Cai, S. Y. Wang, S. J. Ji, *Org. Lett.*, 2013, **15**, 5226-5229; (c) Y. Zi, Z. J. Cai, S. Y. Wang, S. J. Ji, *Org. Lett.*, 2014, **16**, 3094–3097.

6 (a) Y. L. Zhong, F. Peng, F. Bao, S. Y. Wang, X. Y. Ji, L. Yang, Y. Y. Su, S. T. Lee, Y. He, *J. Am. Chem. Soc.*, 2013, **135**, 8350-8356; (b) Y. L. Zhong, X. T. Sun, S. Y. Wang, F. Peng, F. Bao, Y. Y. Su, Y. Y. Li, S. T. Lee, Y. He, *ACS Nano*, 2015, **9**, 5958-5967.

7 M. Li, S. K. Cushing, X. Zhou, S. Guo, N. Wu, *J. Mater. Chem.*, 2012, **22**, 23374–23379.

8 X. Wang, L. Cao, S. T. Yang, F. S. Lu, M. J. Meziani, L. L. Tian, K. W. Sun, M. A. Bloodgood, Y. P. Ya, *Angew. Chem. Int. Ed.*, 2010, **49**, 5310–5314.

9 J. Andres, R. D. Hersch, J. E. Moser, A. S. Chauvin, *Adv. Funct. Mater.*, 2014, **24**, 5029-5036.

View Article Online
DOI: 10.1039/C8CC00047F

Table of Contents

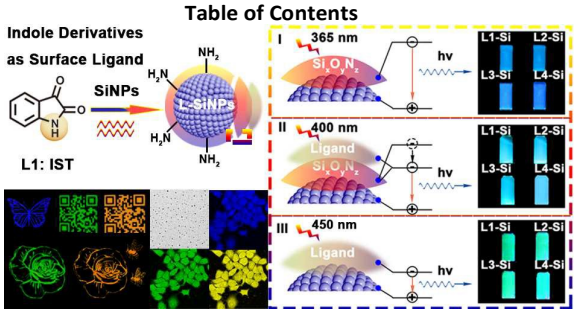

Rational introduction of surface ligand leads to the production of SiNPs with excitation-wavelength-dependent fluorescence.